

Artificial Cells, Nanomedicine, and Biotechnology

An International Journal

ISSN: (Print) (Online) Journal homepage: www.tandfonline.com/journals/ianb20

Antibacterial, antioxidant, and haemolytic potential of silver nanoparticles biosynthesized using roots extract of *Cannabis sativa* plant

Suman Suman, Lacy Loveleen, Meena Bhandari, Asad Syed, Ali H. Bahkali, Romila Manchanda & Surendra Nimesh

To cite this article: Suman Suman, Lacy Loveleen, Meena Bhandari, Asad Syed, Ali H. Bahkali, Romila Manchanda & Surendra Nimesh (2022) Antibacterial, antioxidant, and haemolytic potential of silver nanoparticles biosynthesized using roots extract of *Cannabis sativa* plant, *Artificial Cells, Nanomedicine, and Biotechnology*, 50:1, 343-351, DOI: [10.1080/21691401.2022.2149543](https://doi.org/10.1080/21691401.2022.2149543)

To link to this article: <https://doi.org/10.1080/21691401.2022.2149543>



© 2022 The Author(s). Published by Informa UK Limited, trading as Taylor & Francis Group



Published online: 15 Dec 2022.



Submit your article to this journal [↗](#)



Article views: 1907



View related articles [↗](#)



View Crossmark data [↗](#)



Citing articles: 1 View citing articles [↗](#)

Antibacterial, antioxidant, and haemolytic potential of silver nanoparticles biosynthesized using roots extract of *Cannabis sativa* plant

Suman Suman^a, Lacy Loveleen^b, Meena Bhandari^a, Asad Syed^c, Ali H. Bahkali^c, Romila Manchanda^{a,d} and Surendra Nimesh^b

^aDepartment of Chemistry, School of Basic and Applied Sciences, K.R. Mangalam University, Gurugram, India; ^bDepartment of Biotechnology, School of Life Sciences, Central University of Rajasthan, Ajmer, India; ^cDepartment of Botany and Microbiology, College of Science, King Saud University, Riyadh, Saudi Arabia; ^dThe Institute for Quantitative Health Science and Engineering, Michigan State University, East Lansing, MI, USA

ABSTRACT

In this study, *Cannabis sativa* roots extract has been employed for the biosynthesis of silver nanoparticles (AgNPs). The appearance of reddish-brown colour followed by absorption peak of AgNPs at 408 nm through UV-vis spectrophotometry suggested biosynthesis of AgNPs. The size of the particles ranged from 90–113 nm, confirmed using DLS and TEM along with zeta potential of -25.3 mV. The FTIR provided information regarding the phytochemical capping. The study was further elaborated for determining AgNPs antibacterial, antioxidant, and cellular toxicity using MIC, DPPH, MTT, and haemolytic assays, respectively. The AgNPs were significantly effective against *Staphylococcus aureus* (Gram-positive), as compared to that of *Pseudomonas aeruginosa*, *Klebsiella pneumoniae*, and *Escherichia coli* (Gram-negative). AgNPs also exhibited remarkable antioxidant potential wherein $58.01 \pm 0.09\%$ free radical scavenging was observed at a concentration of $100 \mu\text{g/ml}$. AgNPs revealed lower cytotoxicity where cell viability was observed to be $52.38 \pm 0.6\%$ at a very high concentration of $500 \mu\text{g/ml}$ in HEK 293 cells. Further, very low toxicity was seen in RBCs i.e. $6.47 \pm 0.04\%$ at a high concentration of $200 \mu\text{g/ml}$. Thus, the current study beholds anticipation that *Cannabis sativa* ethanolic root extract-mediated AgNPs may play a vital role in therapeutic.

ARTICLE HISTORY

Received 12 September 2022
Revised 14 November 2022
Accepted 16 November 2022

KEYWORDS

Cannabis sativa; silver nanoparticles; antibacterial; antioxidant; cytotoxicity





Introduction

Nanotechnology empowers manipulation of substances at their atomic and molecular level, creating products with marvellous properties. Over time, nanotechnology has taken roots in myriads of fields such as scientific research, agriculture, medicine, pharmaceuticals, catalysis, optics, and other food and textile industries [1]. Nanoparticles are particles having at least any one of their dimensions ranging in nanoscales (1–100nm) [2]. These particles derive their uniqueness from the elements from which they are made and the materials that they carry. Based on shape, size, and composition they can be categorized as polymeric, ceramic, fullerenes, and metallic nanoparticles [3]. Among all the engineered nanoparticles available, the novel metallic nanoparticles are the most explored and intensively investigated. Silver nanoparticles (AgNPs) seem to be the most crowd-pleasing because of their strong surface plasmon resonance (SPR) at a shorter wavelength, minimum loss of absorption intensity, and cost-effectiveness [4].

The synthesis of nanoparticle employs two general mechanisms: the top-down and the bottom-up approach. The top-

down approach of nanoparticles formation includes the mechanical (laser/thermal ablations, ball milling, etc.) and some of the chemical methods such as chemical leaching. On the other hand, the bottom-up approach accompanies the biological method using plant parts, algae, bacteria and fungi as source of nanoparticles formation along with some of the chemical methods (spray pyrolysis, chemical decomposition, aerosol process, etc) [5]. Thus, the phytochemical-mediated green synthesis of AgNPs using a bottom-up approach is employed due to their low toxicity, robustness, eco-friendliness, and affordability [6]. The plant extracts contain several metabolites, amongst them some act as reducing agents while some as capping agents for AgNPs [7]. Several studies have been conducted so far on the biosynthesis of AgNPs using plant extract that includes *Terminalia arjuna* [8] and *Prosopis juliflora* bark [9], *Canarium ovatum* [10], *Cordia dichotoma* [11] and *Punica granatum* leaf [12], orange peels [13], *Putranjiva roxburghii* Wall. seed [14], leaves of *Eucalyptus globulus* [15], *Azadirachta indica* [16] and *Brassica oleracea* [17] and many other such plants.

In this investigation, the ethanolic root extract of *Cannabis sativa*, commonly known as, Marijuana or Hemp, has been

CONTACT Romila Manchanda  manchan7@msu.edu  The Institute for Quantitative Health Science and Engineering, Michigan State University, Bandsindri, N.H. 8, Teh-Kishangarh, Dist, East Lansing, 48824, MI, USA; Surendra Nimesh  surendranimesh@gmail.com  Department of Biotechnology, School of Life Sciences, Central University of Rajasthan, Ajmer, 305817, Rajasthan, India

© 2022 The Author(s). Published by Informa UK Limited, trading as Taylor & Francis Group
This is an Open Access article distributed under the terms of the Creative Commons Attribution License (<http://creativecommons.org/licenses/by/4.0/>), which permits unrestricted use, distribution, and reproduction in any medium, provided the original work is properly cited.

used for the synthesis of silver nanoparticles. *Cannabis* belongs to the family *Cannabaceae*, and is a cosmopolitan herbaceous plant, originating from Central Asia. For millennia, *Cannabis* has been used for the treatment of pain, insomnia, spasm, asthma, depression and anorexia. Cannabinoids, terpenoids, sterols and flavonoids are some of the common secondary metabolites of the plant that have substantially contributed towards its therapeutic potential and for the biosynthesis of AgNPs [18]. Herein, the AgNPs synthesis has been performed through optimization of reaction parameters mainly concentration of silver nitrate salt (AgNO_3), temperature, volume of root extract, and pH, of the reaction [19]. Further, the antibacterial property of the extract was checked against Gram-negative (*Escherichia coli*, *Pseudomonas aeruginosa* and *Klebsiella pneumoniae*) and Gram-positive (*Staphylococcus aureus*) bacterial species. The study also highlights the antioxidant, and reduced haemolytic properties of AgNPs against the HEK 293 cells and human RBCs.

Materials and methods

Materials

Silver nitrate was purchased from HiMedia Chemicals, India. 3-(4,5-dimethyl-2-thiazolyl)-2,5-diphenyltetrazolium bromide (MTT), Dulbecco's Modified Eagle's Medium-high glucose (DMEM-HG), Triton-X 100, sodium borohydride (NaBH_4) and p-nitrophenol were procured from Sigma Aldrich Co., St. Louis, MO. 1,1-Diphenyl-2-picrylhydrazyl (DPPH) was obtained from TCI Chemicals, India.

Cell cultures

HEK 293 cells for cell culture experiments were purchased from ATCC, India. The Gram-positive bacterial strains (*S. aureus*) and Gram-negative bacterial strains (*E. coli*, *P. aeruginosa*, and *K. pneumoniae*) were grown in media at 37 °C and stored at -70 °C in Brain Heart Infusion (BHI) broth containing 40% glycerol.

Plant identification and sampling

Cannabis sativa roots were collected locally from Gurugram, Sector 47, Haryana, India and identified. The roots were firstly washed with tap water for the removal of dirt and other impurities followed by cleansing through distilled water. Further, the roots were shade dried for one month. The dried roots were then milled to fine powder.

Ethanollic root extract preparation

A total of 15g of dried root powder was mixed with 100 ml of ethanol on magnetic stirrer (UC152, Stuart, UK) for 1 h. The mixture was then evaporated on vacuum rotary evaporator (Hei-VAP precision, Heidolph GmbH & Co KG, Germany). Further, the residue was mixed with 100 ml of distilled water and boiled at 85 °C for 2 h with continuous stirring on same

magnetic stirrer. The extract was cooled down to room temperature for 4 h, before centrifugation. The suspension was then centrifuged at 10,000rpm for 10 min at room temperature. The filtrate obtained using gravity filtration was stored at 4 °C, for the forthcoming reactions.

Biological synthesis of silver nanoparticles

A total of 5 ml of root extract was dripped to 45 ml of freshly prepared AgNO_3 solution with continuous stirring at 85 °C. The reaction processed till the colour of the solution changed from yellow to reddish brown. The obtained reaction mix was thereafter centrifuged for 15 min at 10,000 rpm for obtaining silver nanoparticles pellet. These pellets were then washed with Milli Q water thrice. The pellets obtained were thereafter vacuum dried to get powdered nanoparticles for further physicochemical evaluation.

UV-visible spectrophotometer analysis

The synthesis of AgNPs was confirmed by scanning the absorbance peak from 200-600nm using UV-visible spectrophotometer (Cary60S UV-vis spectrophotometer, Agilent Technologies, Santa Clara, CA), due to characteristic SPR of AgNPs peak ranging between 400-450nm.

Optimization of the reaction variables

The green synthesis of silver nanoparticles requires mild and optimum temperature, change in optimal conditions may lead to quality compromised particles having variable size, shape, and yield. The parameters governing the reaction such as temperature, concentration of AgNO_3 , volume ratio of *Cannabis sativa* root extract to AgNO_3 and pH were accessed to achieve the optimum nanoparticle size. The reaction was performed at variable temperatures that is, 85 °C, 75 °C, 65 °C, 55 °C and 45 °C, followed by volume ratios of 1:0.5, 1:1, 1:5, 1:10 and 1:20, concentration of silver nitrate solutions as 0.5 mM, 1 mM, 1.5 mM and 2 mM and pH ranging from 6-10, keeping one of the parameters as variable and others fixed at a given point of time.

Silver nanoparticles stability assessment

The ability of nanoparticles to preserve their morphological properties such as size, surface chemistry and shape by protecting themselves from decomposition, aggregation, crystallization, and adulteration by similar materials is known as nanoparticles stability. The more the particles are stable, the more time they can be stored and utilized. The nanoparticles stability solely depends on the target size, shape and property [20]. The stability of nanoparticles was analysed again after 6 months of storage at room temperature.

Characterization of nanoparticles

The freshly prepared silver nanoparticles were subjected to characterization through various techniques for determining

their, distinctive absorption peak, hydrodynamic size, shape, surface charge, and capping agents. Dynamic light scattering and Zeta potential were used for examining the hydrodynamic radius, surface electric charge and polydispersity index of AgNPs. The Brownian movement of particles dispersed in the solvent are utilized for the determination of size distribution of the colloids [21,22]. The surface charge is analysed by electrophoretic mobility of charged particles present in colloidal suspension under an applied electric potential using Zetasizer, Nano ZS (Malvern instruments, UK) applying a nominal 5mW He-Ne laser operating at a wavelength of 633 nm. Ultrapure water having refractive index (1.33) and the viscosity (0.89) was used at 25 °C for measurements, and the scattering of light was detected at an angle of 173°. The nanoparticles size and zeta potential were measured as an average value of 30 runs. The technique can also determine the stability of AgNPs [23].

The morphological scrutinization of the silver nanoparticles were performed using HRTEM (Tecnai G2, FEI, Holland) operating at 200 kV. The atomic-resolution real-space imaging is one of the key feature of TEM, hence utilized for precise morphology of nanoparticles [24]. Thereafter, the phytochemicals adhered over the AgNPs for their reduction and stabilization were analysed using Fourier Transmission Infra-red Spectroscopy. FTIR spectra of root extract and AgNPs was recorded on a single beam Perkin Elmer Spectrum (BX Series) in the range of 4000 cm⁻¹ to 400 cm⁻¹ at 4 cm⁻¹ resolution [25].

Estimation of minimum inhibitory concentration and antibacterial activity

The minimum concentration of an antimicrobial agent that can inhibit the visible growth of organisms after overnight incubation is termed as minimum inhibitory concentration (MIC) [26]. The current study investigated the MIC of AgNPs against both Gram-positive (*S. aureus*) and Gram-negative (*E. coli*, *P. aeruginosa* and *K. pneumoniae*) bacteria. The experiment was performed in 96-well plate by using microbroth dilution assay. Certain concentrations (2, 5, 10, 25, 50, 100 and 200 µg/ml) of AgNPs were added to 10 µl of bacterial culture and Mueller Hinton Broth (HiMedia) solution. Finally, the volume of each well was made up to 200 µl. The microtiter plate was incubated overnight at 37 °C. Absorbance was recorded at 600 nm before and after incubation period using TECAN spectrophotometer. Subsequently, in each well about 50 µl of 200 µg/ml of p-iodonitrotetrazolium chloride (INT) was added and again incubated for 30 min at 37 °C to analyse bacterial growth.

The antimicrobial activity of synthesized AgNPs was observed against both Gram-positive and Gram-negative bacteria using method as mentioned by [27]. The bacterial strains were cultured in LB media at 37 °C. Gentamycin (0.01 mg/ml) was used as positive control and Milli Q water was used as negative control. Inoculum of optical density 0.5 was prepared by using 1 × 10⁵ CFU/ml. The AgNPs of varying concentration (25, 50, 100, 200 µg/ml) were added to observe antimicrobial activity. Experiment was carried in 96-well microtiter plate and further incubated at 37 °C. After 24 h,

absorbance was recorded at 600 nm and % survival of bacterial strains was measured.

Evaluation of antioxidant activity using DPPH assay

The antioxidant activity of the AgNPs was measured using 2,2-Diphenyl-1-picrylhydrazyl (DPPH) assay. The free radicals generated by test samples are scavenged by DPPH with visible colour change of the solution from purple to yellow. 3.9432 mg of DPPH was dissolved in 100 ml of methanol (0.1 mM) to prepare a stock solution which was then stored at 4 °C until use. 2 ml of DPPH solution was added to 1 ml of the synthesized nanoparticles at a range of concentration of 20–100 µg/ml. The reference standard of the experiment was preferably set to 100 µg/ml of ascorbic acid. 1 ml of distilled water mixed with 2 ml of DPPH solution was referred as the control. The reaction mixture was incubated in dark at room temperature for 30 min. The absorbance of the sample was recorded at 517 nm. The antioxidant activity of the AgNPs was calculated by the following equation [28]:

$$\text{Scavenging \%} = \left(\frac{A_{\text{control}} - A_{\text{sample}}}{A_{\text{control}}} \right) \times 100$$

Evaluation of haemolytic activity

The toxicity assessment of AgNPs on red blood corpuscles was observed by using the haemolytic assay. Fresh human blood sample was collected in EDTA tubes from the healthy subject from an authorized lab. Blood sample was centrifuged at 2000 rpm for 10 min at 4 °C for serum separation. The precipitate was washed thrice with 1 × PBS (pH 7.4). The RBC pellets were collected and dispersed in PBS solution to make 4% RBC suspension. Different concentration of AgNPs (5, 10, 25, 50, 100, 150 and 200 µg/ml) were added in a 96-well plate and diluted to 100 µl with 1 × PBS solution. Further, 100 µl of 4% suspension of RBCs were added to the wells having AgNPs and Triton-X (0.1%, v/v) was referred to as a positive control. The plate was then incubated for 1 h at 37 °C and centrifuged at 800 g for 10 min at 4 °C. Subsequently, the supernatant (100 µl) was transferred to 96-well plate. By using ELISA plate reader, absorbance was measured at 540 nm. The haemolysis (%) was calculated by using the equation [29]:

$$\text{Haemolysis \%} = A_{\text{sample}} - \frac{A_{\text{PBS}}}{A_{\text{Triton-X}}} \times 100$$

Estimating the percentage cell viability of HEK 293 and human RBCs

The cytotoxicity of AgNPs was observed on mammalian cell line, HEK 293 (Human Embryonic Kidney 293). The HEK cells were harvested under standard condition of 37 °C and 5% CO₂. The harvested cells with a density of ~1 × 10⁴ cells per well were seeded to 96 well plates (100 µl/well) and further incubated for 12 h at 37 °C. Further, different concentration of AgNPs (50, 100, 200, 300, 500 µg/ml) were added into the

wells seeded with HEK cells and incubated for 24 h at 37 °C in a CO₂ incubator. The cells were separated from the supernatant and rinsed with 1 × PBS solution. Then 100 µl MTT solution (1.0 mg/ml) was poured in to each well of the plate and incubated for 3 h. In the post-incubation period, the supernatant was aspirated. The variable cells formed formazan crystals by reducing the MTT. These crystals were then dissolved by treatment with 100 µl of dimethyl sulfoxide. The solution without AgNPs was used as control. The well plate recipients were transferred to microplate reader and the absorbance (optical density (OD) of each well was measured at 540 nm. The observed absorbance was used to calculate cell viability by using the equation [30]:

$$\text{Cell viability} = 1 - \left(\frac{\text{OD}_{\text{control}} - \text{OD}_{\text{well}}}{\text{OD}_{\text{control}}} \right) \times 100$$

Results and discussions

Biological synthesis of silver nanoparticles

The biosynthesis of silver nanoparticles was conducted under controlled conditions as 85 °C temperature, 1 mM AgNO₃ concentration, volume of *Cannabis sativa* root extract to AgNO₃ was kept 1:10 with pH 7. As the reaction preceded, the pale-yellow colour of solution was converted to reddish brown colour, visually confirming the formation of AgNPs. As the Ag⁺ were reduced to Ag⁰, the colour of solution changed from pale yellow to reddish brown in colour. Once, the reaction has been performed, the AgNPs were washed and pelleted down, for further analysis.

UV-vis spectrophotometric analysis

The foremost qualitative analysis of silver nanoparticles is done through UV-vis spectrophotometry. The laser beam excites the conduction band electrons, by virtue of which plasmonic resonance occur. The intensity, shape and position of the spectra is however dependent on the surface adsorbed particles, dielectric constant of media and the morphology of the particle. Thus, the particles of different size formed or agglomerated can be detected through the spectra. The spherical shaped nanoparticles show single absorption peak, while the ellipsoidal one shows double peaks [4]. Similarly, sharper peaks indicate the formation of monodispersed nanoparticles while particles with broader and stronger plasmonic peaks shows agglomeration or large sized particles, though if the peak is broader and still weak it may be due to the partially reduced silver [31]. In this study, the synthesized silver nanoparticles due to their characteristic optical properties showed absorbance at 408 nm, with broader peak indicating large size distribution of the particles (Figure 1). The resulting peak is in accordance to the Mie theory, that suggests single absorption peak for particles with spherical shape, and more than one for particles with different shapes [32]. Mahadevan et al. had synthesized silver nanoparticles coated with Chitosan giving absorbance at 419 nm [33]. Similar study was performed by Arya et al. for the biosynthesis silver nanoparticles from *Prosopis juliflora*

bark extract. The AgNPs formed were spherical in shape and gave absorption peak at 420 nm [9].

Physicochemical characterization of silver nanoparticles

The DLS data provides information about the average size of particles, while TEM gives the qualitative i.e. visual representation of the particles such as the shape, size and morphology in which the particles are arranged. The average hydrodynamic size distribution was found to be 90–113 nm. The result of TEM suggests the average size of nanoparticles are 17 nm and the shape of silver nanoparticles was spherical as shown in Figure 2. The stability and surface charge over the AgNPs were inspected by calculating the zeta potential. The colloidal particles are attracted towards the oppositely charged electrodes. Such an electrophoretic mobility of particles determines the size and charge of particles. The study suggested that, the synthesized silver nanoparticles were negatively charged an average value of –25.3 mV, hence, the repulsive force among the particles would not allow them to aggregate, consequently increasing the stability. The negatively charged AgNPs have more binding affinity towards the affinity of bacterial lipid monolayer, increasing the surface pressure. The author further suggests that adsorption of AgNPs was possible probably due to the interaction of the capping agent over the surface of bacteria, inserting the negatively charged AgNPs into the cell membrane [34]. Although, many studies have been reported in support of positively charged nanoparticles to be better antibacterial agents, but the studies conducted by Galbiati et al. propounded the low toxicity of negatively charged silver nanoparticles over mammalian cells as compared to neutral and positively charged nanoparticles, without compromising the antibacterial effects [35]. The role of functional groups of phytochemicals involved in capping of silver nanoparticles has already been highlighted in many studies. Hence, the functional groups of phytochemicals available in the ethanolic root extract of *Cannabis sativa* and those adhered to the surface of AgNPs has been spotted in this study using FTIR as shown in Figure 3. The FTIR analysis of root extract showed the sharp band of high intensity at 3226 cm⁻¹ indicating the O–H stretching vibrations. The peak at 2860 cm⁻¹ shows the C–H stretching indicating the presence of alkanes and less intense band at 2252 cm⁻¹ shows the C–N stretching vibration. The band at 1437 cm⁻¹ represents C–H asymmetric bending and at 1200 cm⁻¹ indicated C–H bending aromatic in plane. Band at 1058 & 852 cm⁻¹ shows C–N stretching vibration indicating the presence of amines and amide groups as shown in Figure 5. Further, bands at 815, 712 and 655 cm⁻¹ shows the =C–H bending in aromatic groups. The AgNPs FTIR spectra shows O–H stretching band at 3300 cm⁻¹. The C=O stretching was observed at 1641 cm⁻¹. Further, peaks at 768, 721 and 663 cm⁻¹ showed the presence of =C–H bending aromatic groups. These various functional groups present in plant extract are found to be responsible for reduction and capping of silver nanoparticles. The peak at 3226 cm⁻¹ in root extract shifted to 3300 cm⁻¹ with slight change in intensity that may be due to

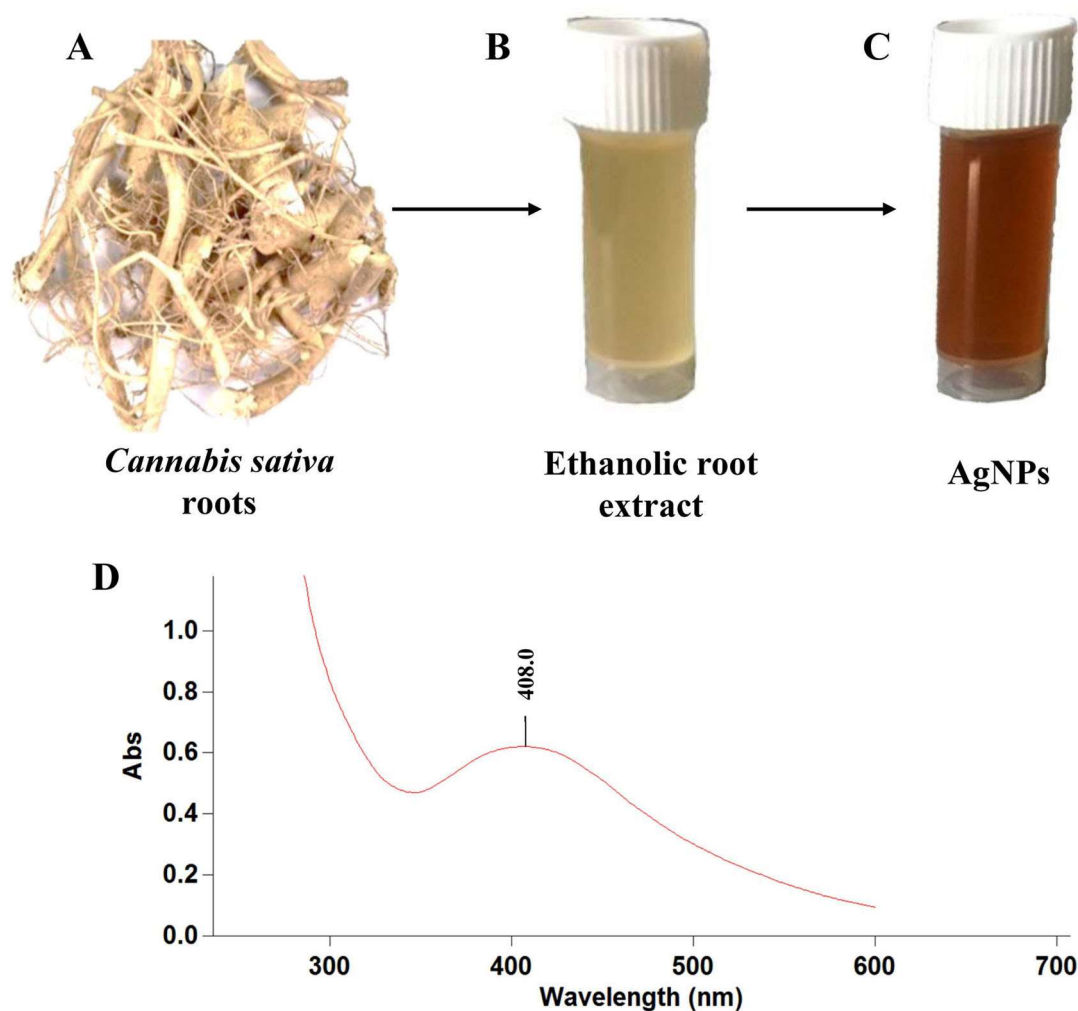


Figure 1. A-*Cannabis sativa* roots, B-*Cannabis sativa* ethanolic roots extract, C-AgNPs synthesized using roots extract, D-UV-vis spectrum of the biosynthesized AgNPs.

intramolecular bonding. The band at 1437 , 1200 and 1058 cm^{-1} of root extract had disappeared and a new band at 1641 cm^{-1} had appeared in AgNPs spectra. Similar functional group analysis were reported by other authors as well in their studies, where FTIR was performed for ethanolic extract of fenugreek leaves and aqueous extract of *Cannabis sativa* hurds, respectively [36,37].

Silver nanoparticles stability assessment

The stability of nanoparticles was analysed using UV-vis spectrophotometer after 6 months of synthesis. The absorbance shifted to longer wavelength at 419 nm as depicted in Figure 4. Such shift of spectra towards the left or red spectrum is known as red shift/Bathochromic shift. The shift may be due to the aggregation of particles with time, however, there is still a single peak indicating the shape of particles has not changed.

Estimation of minimum inhibitory concentration and antibacterial activity

As discussed earlier, the minimum amount of ethanolic root extract mediated silver nanoparticles that could decrease the

bacterial growth significantly was calculated as the MIC values for the given bacterial strains. The zone of inhibition and MIC values are inversely related, less the MIC, more the cell death has occurred, the more is the zone of inhibition [38]. The minimum inhibitory concentration of AgNPs against Gram-positive (*S. aureus*) was found to be $65\text{ }\mu\text{g/ml}$, while in Gram-negative (*E. coli*, *P. aeruginosa* and *K. pneumoniae*) bacteria, it was $70\text{ }\mu\text{g/ml}$, $75\text{ }\mu\text{g/ml}$ and $60\text{ }\mu\text{g/ml}$, respectively, as shown in Figure 5. The result indicated that the synthesized nanoparticles were affecting the Gram-positive bacteria more as compared to Gram-negative, although the cell wall of Gram-positive bacteria are thicker. Similarly, the % cell survival was calculated to be highest (22.77%) in *P. aeruginosa* and least (4.58%) in *E. coli* at highest concentration of $200\text{ }\mu\text{g/ml}$. At minimum concentration of AgNPs, the cell viability of *P. aeruginosa* remains highest (96.58%), followed by *E. coli* (93.63%), *S. aureus* (79.42%) and *K. pneumoniae* (78.28%). In accordance to our study, several authors have reported similar results. The PJB-AgNPs synthesized using the bark extract of *Prosopis juliflora* was found be effective in killing the Gram-negative strains, though more toxic towards *E. coli* than that of *P. aeruginosa* [9]. $15.62\text{--}1000\text{ }\mu\text{g/ml}$ of silver (I) oxide decorated graphene oxide nanocomposite ($\text{Ag}_2\text{O}/\text{GO}$) has been developed exhibiting antimicrobial activity

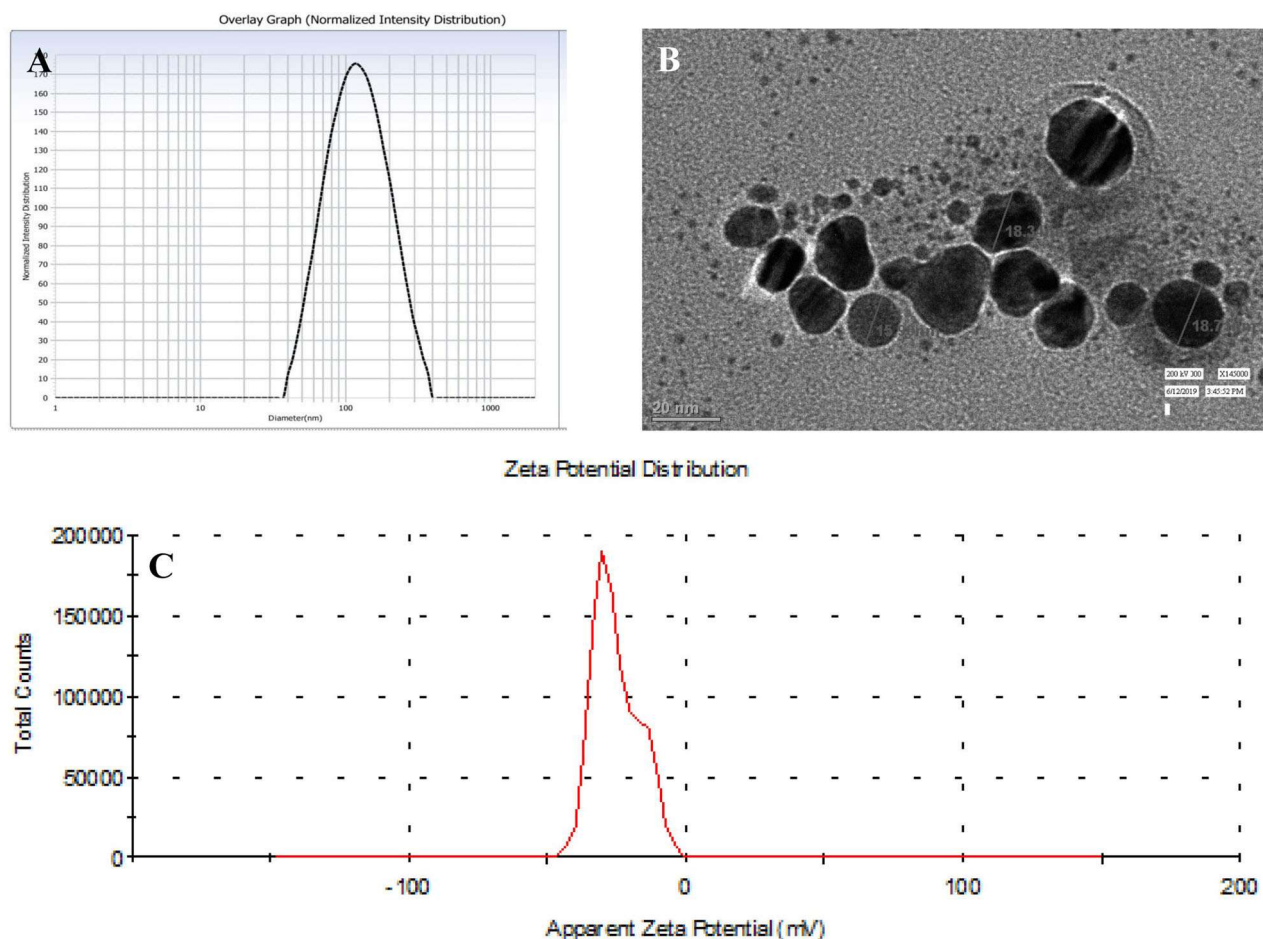


Figure 2. A-DLS spectrum of AgNPs, the size of nanoparticles was in the range of 90–113 nm, B-TEM image of AgNPs, the average size of the nanoparticles is 17 nm, C-Zeta potential of AgNPs, the zeta potential here is -25.3 mV.

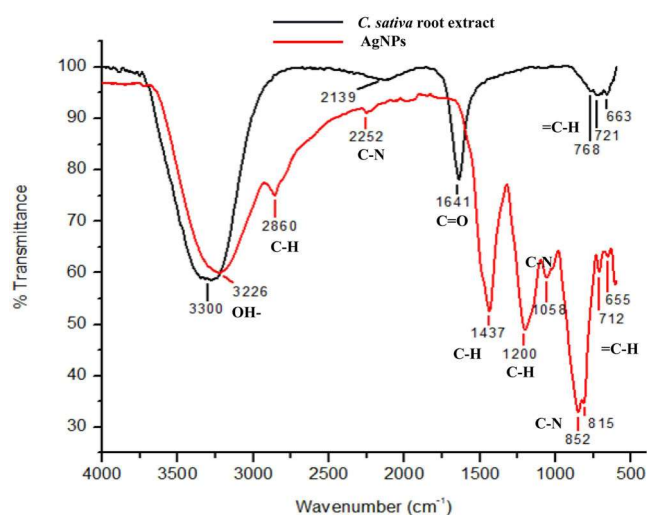


Figure 3. FT-IR spectra of *Cannabis sativa* roots extract and biosynthesized AgNPs depicting major functional groups.

against *S. aureus*, *P. aeruginosa*, *K. pneumoniae*, and *E. coli* with minimum inhibitory concentration of 125 $\mu\text{g}/\text{mL}$ for *P. aeruginosa* and *K. pneumoniae*, and 62.5 $\mu\text{g}/\text{mL}$ for *E. coli*. The maximum MIC was reported for *S. aureus* (250 $\mu\text{g}/\text{mL}$) [39]. The probable mechanisms may be the interaction of silver nanoparticles with the thiol ($-\text{SH}$) groups of cysteine present

in bacterial proteins. This inhibits the respiratory mechanism of bacteria, hence leading to cell death. Once the AgNPs are inserted, they may cause DNA damage, over produce ROS, by arresting the free radical scavenging mechanism of the bacteria. In a study conducted using chitosan-mediated synthesis of silver nanoparticles, it was observed that the AgNPs were highly effective against the *Methicillin-resistant Staphylococcus aureus* (MRSA), *E. coli* and *P. aeruginosa* with zone of inhibition 39 mm, 38 mm and 36 mm, respectively [33]. Other studies report the disruption of first line of defence, the cell wall, to be the main reason of bacterial cell death. Studies suggest that the phytochemicals may first interact with the negatively charged bacterial cell walls creating pores leading to insertion of AgNPs into the cell [34]. It may be concluded that, biosynthesized nanoparticles are potential antibacterial agents, when applied with increasing concentration gradient.

Evaluation of antioxidant activity using DPPH assay

The natural phytochemicals such as polyphenols and flavonoids are present in abundance in plants to protect plant against the bacterial aggregation and harmful UV radiations. These dietary polyphenols contribute greatly to human health by acting as excellent antioxidants [40]. The polyphenols and flavonoids present in *Cannabis sativa* also contribute in a

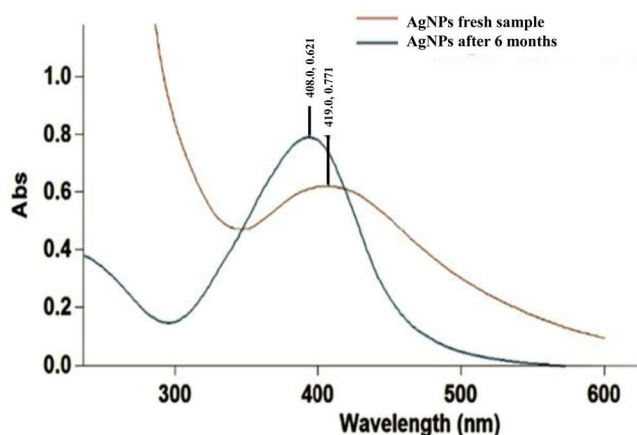


Figure 4. UV-vis spectra of AgNPs at different time points, i.e. fresh after bio-synthesis and after storage for 6 months at room temperature; done to study the stability of biosynthesized AgNPs.

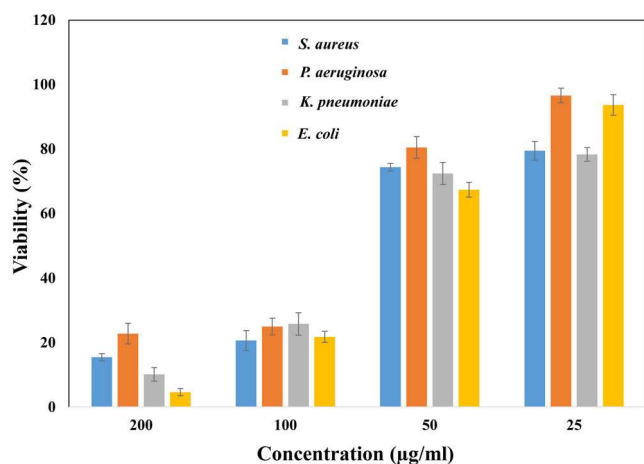


Figure 5. Antibacterial activity of AgNPs by broth dilution method against Gram positive and Gram negative bacteria. The bacterial cell viability decreased with increased in concentration of AgNPs.

similar way to reduce the oxidizing nature of AgNPs [18]. Thus, the addition of such compounds using green synthesis method, reducing toxicity over eukaryotic cell lines. In this study, ascorbic acid, had the maximum free radical scavenging ability, followed by biosynthesized AgNPs and ethanolic root extract of *Cannabis sativa*, in dose dependent manner (20, 40, 60, 80, 100 µg/ml) with respect to free radicals generated by DPPH[•]. At highest concentrations, the % free radical scavenging capacities of ascorbic acid, AgNPs and root extract are 77.96%, 58.01%, and 24.82%, respectively. Similarly, at minimum concentrations of ascorbic acid, AgNPs and root extract, the free radical scavenging capacity decrease to 22.93%, 13.99%, and 9.02%, respectively, with reference to Figure 6. The antioxidant property of chitosan-silver nanoparticles represented similar results, providing evident free radical scavenging property of AgNPs [33,41]. However, the leaf extract of *Cannabis sativa* has been reported to have more free radical inhibition property in comparison to the silver nanoparticles synthesized using the same [42]. The obtained results recommend the application of AgNPs as useful natural antioxidants and can be used against oxidative stress associated with degenerative diseases for health benefits.

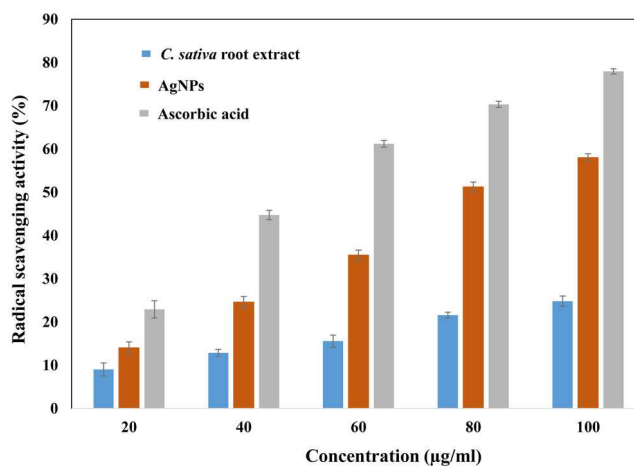


Figure 6. Antioxidant efficacy of AgNPs estimated using DPPH assay at different concentrations of nanoparticles. The nanoparticles showed comparative radical scavenging to ascorbic acid.

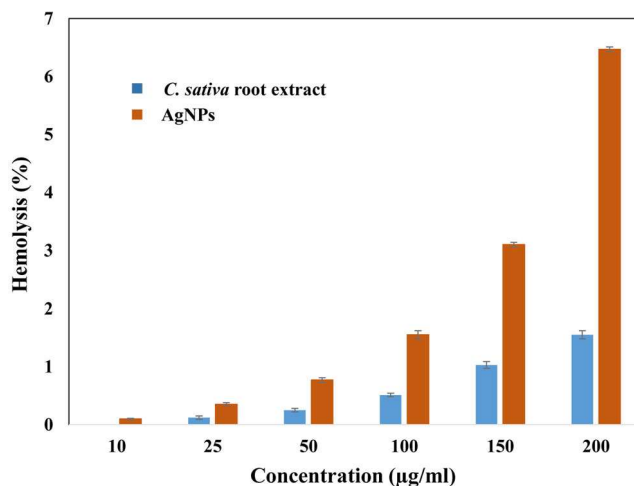


Figure 7. Haemolytic activity of AgNPs done employing human RBC. Higher haemolysis was seen at higher concentration of AgNPs.

Evaluation of haemolytic activity

Nanomaterials enters the body and ultimately meets the circulatory system. The blood cells, being an important component of our body, needs to be carefully dealt with the exogenous particles they are interacting. The *Cannabis sativa* root extract and synthesized silver nanoparticles were examined against human RBCs at different concentrations of 5, 10, 25, 50, 100, 150 and 200 µg/ml. In Figure 7, the highest % haemolysis was found to be $1.55 \pm 0.07\%$ and $6.47 \pm 0.04\%$ at the maximum concentration of plant extract and AgNPs, respectively. At least concentration (10 µg/ml) of plant extract and AgNPs, the % haemolysis also decreased to 0% and 0.1%, respectively. The haemolytic activity of AgNPs and root extract were also tested at 5 µg/ml, and fortunately none of the cells were lysed. The haemolytic activity of polymeric nanoparticles was analysed in some of the studies, suggested, that polymeric nanoparticles at concentration of 40 µg/ml causes haemolysis of $>10\%$ [43]. The ethanolic extract of *Cannabis sativa* has plant extract has been reported by other authors as well. They found that the haemolytic activity (%) was insignificant ranging from 1.97 to

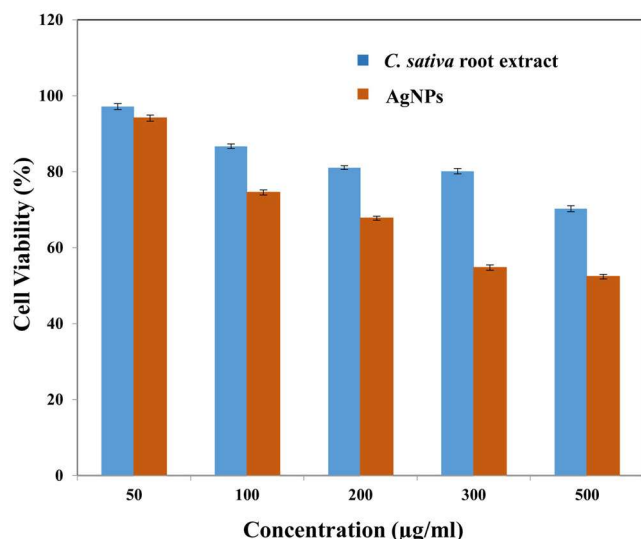


Figure 8. Cell viability of HEK 293 cells treated with different concentrations of biosynthesized AgNPs, investigated using MTT assay. The cell viability was observed to reduce at very high concentration of AgNPs (i.e. 200–500 µg/ml).

5.88 [44]. The haemolytic activity was even less (<5%) for silver nanoparticles synthesized using fenugreek and papaya leaves [45]. Thus, our study suggests the haemolytic activity was comparatively less and hence may be employed in biomedical applications.

Estimating the percentage cell viability of HEK 293

The nanoparticles administered into an organism, not only makes contact with erythrocytes, but also with other cell and tissues of the body. In this study, human embryonic kidney 293 cells were taken into consideration for cell viability evaluation. The cells were exposed to different concentrations (50, 100, 200, 300, 500 µg/ml) of plant extract and silver nanoparticles. It was ascertained that, at highest concentration of both plant extract and silver nanoparticles the cellular viability was minimum, $70.27 \pm 0.8\%$ and $52.38 \pm 0.6\%$, respectively. At concentration 50 µg/ml, maximum cells survived were $97.17 \pm 0.8\%$ in case of plant extract and $94.13 \pm 0.8\%$ on exposure to AgNPs as shown in Figure 8. Studies have revealed the genotoxic behaviour of AgNPs on HEK 298 cells along with biomechanical changes, in correlated manner [30]. The results are consistent with other reports wherein authors synthesized silver nanoparticles from *Artemisa tournefortiana* extract and examined their cytotoxic effect on human colon cancer (HT 29) and normal HEK 293 cells [46].

Conclusions

The study demonstrates the efficient biosynthesis of silver nanoparticles using *Cannabis sativa* ethanolic root extract. The potency of the plant extract and phytochemically fabricated silver nanoparticles were analysed over certain parameters such as antimicrobial, antioxidant and cellular toxicity tests. The study concludes the significant effectiveness of silver nanoparticles, thus prognosticating their use henceforth.

Acknowledgements

The authors are gratefully thankful to Mr. Pradeep Kumar; CSIR-Institute of Genomics and Integrative Biology, Mall Road, Delhi for his valuable support. The author (Ali H. Bahkali) extends the appreciation to the Researchers Supporting Project number (RSP-2021/15), King Saud University, Riyadh, Saudi Arabia.

Disclosure statement

No potential conflict of interest was reported by the author(s). The authors alone are responsible for the content and writing of the paper.

Funding

The author (Ali H. Bahkali) extends the appreciation to the Researchers Supporting Project number [RSP-2021/15], King Saud University, Riyadh, Saudi Arabia.

Data availability statement

The data that support the findings of this study are available from the corresponding author, SN, upon reasonable request.

References

- [1] Khandel P, Shahi SK. Mycogenic nanoparticles and their bio-prospective applications: current status and future challenges. *J Nanostruct Chem.* 2018;8(4):369–391.
- [2] Bloemen M. Immunomagnetic separation of bacteria by iron oxide nanoparticles. 2015;
- [3] Khan I, Saeed K, Khan I. Nanoparticles: properties, applications and toxicities. *Arab J Chem.* 2019;12(7):908–931.
- [4] Solati E, Dorrani D. Comparison between silver and gold nanoparticles prepared by pulsed laser ablation in distilled water. *J Clust Sci.* 2015;26(3):727–742.
- [5] Tariq M, Mohammad KN, Ahmed B, et al. Biological synthesis of silver nanoparticles and prospects in plant disease management. *Molecules.* 2022;27(15):4754.
- [6] Irvani S, et al. Synthesis of silver nanoparticles: chemical, physical and biological methods. *Res Pharm Sci.* 2014;9(6):385–406.
- [7] Ahmed S, Ahmad M, Swami BL, et al. A review on plants extract mediated synthesis of silver nanoparticles for antimicrobial applications: a green expertise. *J Adv Res.* 2016;7(1):17–28.
- [8] Ahmed Q, Gupta N, Kumar A, et al. Antibacterial efficacy of silver nanoparticles synthesized employing terminalia arjuna bark extract. *Artif Cells Nanomed Biotechnol.* 2017;45(6):1–9.
- [9] Arya G, Kumari RM, Gupta N, et al. Green synthesis of silver nanoparticles using prosopis juliflora bark extract: reaction optimization, antimicrobial and catalytic activities. *Artif Cells Nanomed Biotechnol.* 2018;46(5):985–993.
- [10] Arya G, Kumar N, Gupta N, et al. Antibacterial potential of silver nanoparticles biosynthesized using canarium ovatum leaves extract. *IET Nanobiotechnol.* 2017;11(5):506–511.
- [11] Kumari RM, Thapa N, Gupta N, et al. Antibacterial and photocatalytic degradation efficacy of silver nanoparticles biosynthesized using Cordia dichotoma leaf extract. *Adv Nat Sci: Nanosci Nanotechnol.* 2016;7(4):045009.
- [12] Singhal M, Chatterjee S, Kumar A, et al. Exploring the antibacterial and antibiofilm efficacy of silver nanoparticles biosynthesized using punica granatum leaves. *Molecules.* 2021;26(19):5762.
- [13] Kahrilas GA, Wally LM, Fredrick SJ, et al. Microwave-assisted green synthesis of silver nanoparticles using orange peel extract. *ACS Sustainable Chem Eng.* 2014;2(3):367–376.
- [14] Nayaka S, Bhat MP, Chakraborty B, et al. Research paper seed extract-mediated synthesis of silver nanoparticles from putranjiva roxburghii wall, phytochemical characterization, antibacterial

- activity and anticancer activity against MCF-7 cell line. *Pharmaceut-Sci.* 2020;82(2):260–269.
- [15] Ali K, Ahmed B, Dwivedi S, et al. Microwave accelerated green synthesis of stable silver nanoparticles with eucalyptus globulus leaf extract and their antibacterial and antibiofilm activity on clinical isolates. *PLoS One.* 2015;10(7):e0131178.
- [16] Haroon M, Zaidi A, Ahmed B, et al. Effective inhibition of phytopathogenic microbes by Eco-Friendly leaf extract mediated silver nanoparticles (AgNPs). *Indian J Microbiol.* 2019;59(3):273–287.
- [17] Rani P, Ahmed B, Singh J, et al. Silver nanostructures prepared via novel green approach as an effective platform for biological and environmental applications. *Saudi J Biol Sci.* 2022;29(6):103296.
- [18] Jin D, Dai K, Xie Z, et al. Secondary metabolites profiled in cannabis inflorescences, leaves, stem barks, and roots for medicinal purposes. *Sci Rep.* 2020;10(1):3309.
- [19] Khalil MM, Ismail EH, El-Baghdady KZ, et al. Green synthesis of silver nanoparticles using olive leaf extract and its antibacterial activity. *Arabian J Chem.* 2014;7(6):1131–1139.
- [20] Phan HT, Haes AJ. What does nanoparticle stability mean? *J Phys Chem C Nanomater Interfaces.* 2019;123(27):16495–16507.
- [21] Han HD, Mangala LS, Lee JW, et al. Targeted gene silencing using RGD-labeled chitosan nanoparticles. *Clin Cancer Res.* 2010;16(15):3910–3922.
- [22] Falke S, Betzel C. Dynamic light scattering (DLS): principles, perspectives, applications to biological samples. *Radiation Bioanal.* 2019;8:173–193.
- [23] Venkata SK, Gaddam SA, Kotakadi VS, et al. Multifunctional silver nanoparticles by fruit extract of terminalia belarica and their therapeutic applications: a 3-in-1 system. *Nano BioMed ENG.* 2018;10(3):279–294.
- [24] Wang ZL. Transmission electron microscopy of shape-controlled nanocrystals and their assemblies. *J Phys Chem B.* 2000;104(6):1153–1175.
- [25] Baudot C, Tan C, Kong J. FTIR spectroscopy as a tool for nanomaterial characterization. *Infrared Phys Technol.* 2010;53(6):434–438.
- [26] Andrews JM. Determination of minimum inhibitory concentrations. *J Antimicrob Chemother.* 2001;48 Suppl 1(Suppl 1):5–16.
- [27] Jha D, Thiruveedula PK, Pathak R, et al. Multifunctional biosynthesized silver nanoparticles exhibiting excellent antimicrobial potential against multi-drug resistant microbes along with remarkable anticancerous properties. *Mater Sci Eng C Mater Biol Appl.* 2017;80:659–669.
- [28] Jadhav MS, Kulkarni S, Raikar P, et al. Green biosynthesis of CuO & Ag–CuO nanoparticles from malus domestica leaf extract and evaluation of antibacterial, antioxidant and DNA cleavage activities. *New J Chem.* 2018;42(1):204–213.
- [29] Evans BC, et al. Ex vivo red blood cell hemolysis assay for the evaluation of pH-responsive endosomolytic agents for cytosolic delivery of biomacromolecular drugs. *J Vis Exp.* 2013;73:e50166.
- [30] Jiang X, Lu C, Tang M, et al. Nanotoxicity of silver nanoparticles on HEK293T cells: a combined study using biomechanical and biological techniques. *ACS Omega.* 2018;3(6):6770–6778.
- [31] Ider M, Abderrafi K, Eddahbi A, et al. Silver metallic nanoparticles with surface plasmon resonance: synthesis and characterizations. *J Clust Sci.* 2017;28(3):1051–1069.
- [32] Kelly KL, Coronado E, Zhao LL, et al. The optical properties of metal nanoparticles: the influence of size, shape, and dielectric environment. *J Phys Chem B.* 2003;107(3):668–677. ACS Publications
- [33] Dara PK, Mahadevan R, Digita PA, et al. Synthesis and biochemical characterization of silver nanoparticles grafted chitosan (Chi-Ag-NPs): in vitro studies on antioxidant and antibacterial applications. *SN Appl Sci.* 2020;2(4):665.
- [34] Ferreyra Maillard APV, Dalmaso PR, López de Mishima BA, et al. Interaction of green silver nanoparticles with model membranes: possible role in the antibacterial activity. *Colloids Surf B Biointerfaces.* 2018;171:320–326.
- [35] Salvioni L, Galbiati E, Collico V, et al. Negatively charged silver nanoparticles with potent antibacterial activity and reduced toxicity for pharmaceutical preparations. *Int J Nanomedicine.* 2017;12:2517–2530.
- [36] Senthil B, Devasena T, Prakash B, et al. Non-cytotoxic effect of green synthesized silver nanoparticles and its antibacterial activity. *J Photochem Photobiol B.* 2017;177:1–7.
- [37] Mandal S, Marpu SB, Hughes R, et al. Green synthesis of silver nanoparticles using cannabis sativa extracts and their anti-bacterial activity. *GSC.* 2021;11(01):28–38.
- [38] Tayung KN, Jha D, Deka DC. Isolation and identification of antimicrobial agent-producing bacterium from taxus baccata rhizosphere antagonistic against clinically significant microbes. *Indian J Microbiol.* 2007;47(4):317–322.
- [39] Khan A, Ameen F, Khan F, et al. Fabrication and antibacterial activity of nanoenhanced conjugate of silver (I) oxide with graphene oxide. *Mater Today Commun.* 2020;25:101667.
- [40] Pandey KB, Rizvi SI. Plant polyphenols as dietary antioxidants in human health and disease. *Oxid Med Cell Longev.* 2009;2(5):270–278.
- [41] Hajji S, Khedir SB, Hamza-Mnif I, et al. Biomedical potential of chitosan-silver nanoparticles with special reference to antioxidant, antibacterial, hemolytic and in vivo cutaneous wound healing effects. *Biochim Biophys Acta Gen Subj.* 2019;1863(1):241–254.
- [42] Csakvari AC, Moisa C, Radu DG, et al. Green synthesis, characterization, and antibacterial properties of silver nanoparticles obtained by using diverse varieties of cannabis sativa leaf extracts. *Molecules.* 2021;26(13):4041.
- [43] Huang H, Lai W, Cui M, et al. An evaluation of blood compatibility of silver nanoparticles. *Sci Rep.* 2016;6(1):25518.
- [44] Shah SB, Sartaj L, Hussain S, et al. In-vitro evaluation of antimicrobial, antioxidant, alpha-amylase inhibition and cytotoxicity properties of cannabis sativa. *Adv Tradit Med (Adtm).* 2020;20(2):181–187.
- [45] Ashokraja C, Sakar M, Balakumar S. A perspective on the hemolytic activity of chemical and green-synthesized silver and silver oxide nanoparticles. *Mater Res Express.* 2017;4(10):105406.
- [46] Movagharnia R, Baghbani-Arani F, Sadat Shandiz SA. Cytotoxicity effects of green synthesized silver nanoparticles on human Colon cancer (HT29) cells. *Feyz J Kashan Univ Med Sci.* 2018;22(1):31–38.